PHYSICAL REVIEW B VOLUME 62, NUMBER 14 1 OCTOBER 2000-II

Influence of aluminum doping and hydrogen disorder on the magnetism of the frustrated Laves hydrides $Y(Mn_{1-x}Al_x)_2H_y$

I. Mirebeau,[1] I. N. Goncharenko,[1,2] D. Andreani,[1] and E. Suard[3]
[1]*Laboratoire Léon Brillouin, CEA-CNRS, CE Saclay, 91191 Gif sur Yvette, France*
[2]*Russian Research Center, Kurchatov Institute, 123182 Moscow, Russian Federation*
[3]*Institut Laue Langevin, Boîte Postale 156, F-38042 Grenoble, France*

(Received 17 April 2000)

We have studied the influence of Al substitution on the crystal and magnetic structure of the Laves hydrides $Y(Mn_{1-x}Al_x)_2H_y$ with maximal hydrogen content ($y=4\pm0.3$). A small amount of Al breaks the magnetic long-range order, which was stabilized in the pure compound $YMn_2H_{4.3}$ by a peculiar hydrogen superstructure. This strong effect of the Al substitution is not directly related to the dilution of the magnetic Mn lattice, but to the onset of hydrogen disorder in the interstitial sites.

I. INTRODUCTION

The intermetallic compounds RMn$_2$ and their hydrides offers many opportunities to study some original aspects of magnetism, such as magnetic instability, local *versus* itinerant character, topological frustration, and quantum fluctuations. They have a Laves structure, where the Mn atoms occupy corner sharing tetrahedra. The antiferromagnetic Mn-Mn interactions are highly frustrated in this triangular lattice. YMn_2 is the most studied so far, showing remarkable anomalies both in the ordered and in the paramagnetic state.[1–4] Below the ordering transition at T_N, the Mn spins order in a complex helical structure with a tetragonal distortion of the unit cell which helps to accommodate the topological frustration. The Mn moments have an itinerant character above T_N, and they become localized below. The magnetic transition is accompanied by a huge lattice expansion. In YMn_2, the high sensitivity of Mn magnetism to interatomic distances comes from the fact that the Mn-Mn first-neighbor distance is close to the critical distance for the occurrence of a spontaneous magnetic moment.[5] This stimulated many studies on the influence of applied pressure and chemical substitution. We focus here on the effects of Mn/Al dilution and hydrogen doping.

In $Y(Mn_{1-x}Al_x)_2$ the dilution of Mn ions by Al ones has drastic consequences on the magnetic properties.[6–8] The lattice expansion induced by Al helps to stabilize the Mn moments. The large energy range of the spin fluctuations points out that the system still remains rather close to the limit of instability.[4,9,10] Al ions also partially release the frustration, by introducing nonmagnetic defects in the frustrated lattice. As predicted within the model of Villain,[11] the localized Mn moments freeze in a spin-glass state.

In the Laves hydrides YMn_2H_y, H doping also stabilizes Mn magnetism by expanding the lattice,[12] but in contrast with Al atoms, hydrogen ones occupy interstitial sites[13,14] and do not make holes in the magnetic lattice. Moreover, H influences the Mn magnetism by making ordered superstructures, which strongly change the Mn environment. In $YMn_2D_{4.3}$, a compound with maximal doping content, we have observed an interesting coupling between a chemical and a magnetic sublattice.[15,16] As the H atoms order, they induce an antiferromagnetic order of the Mn moments, through a single first-order magnetostructural transition. The magnetic order of the Mn moments is long range. Surprisingly, this simple collinear order occurs in the triangular lattice. As shown in Ref. 17, H ordering releases the frustration by making Mn-Mn interactions nonequivalent. Mn pairs having H atoms as near neighbors become ferromagnetic. In the present paper, this peculiar structure will be considered as a reference to study the evolution of Mn and H orders with Al dilution. The substituted hydrides $Y(Mn_{1-x}Al_x)_2H_y$ allow one to study the effect of magnetic dilution in the triangular Mn lattice for Mn-Mn distances well above the instability limit. Up to now, they have been only partly investigated by NMR and magnetic measurements.[18] We have studied the magnetic and hydrogen orders in these compounds by neutron diffraction. We discuss our results in comparison with YMn_2, $Y(Mn_{1-x}Al_x)_2$, and YMn_2H_y.

II. SAMPLE PREPARATION AND CHARACTERIZATION

Several samples $Y(Mn_{1-x}Al_x)_2D_y$ with different Al contents (in the range $0\leqslant x\leqslant 0.3$) were prepared from the intermetallic compounds $Y(Mn_{1-x}Al_x)_2$. These starting compounds were synthesized by arc melting of Y, Mn, and Al (99.9% purity). An excess of 20% Mn was introduced with respect to the nominal Al content, to account for Mn evaporation. The $Y(Mn_{1-x}Al_x)_2D_y$ compounds were exposed under D_2 atmosphere at 273 K and 0.2 bars until the absorption saturates. The deuterium concentration y was determined by measuring the volume of absorbed gas. Deuterium was used instead of hydrogen in order to decrease the incoherent background for the neutron measurements. In this paper, we will speak of hydrogen for simplicity, whatever isotope is considered. The sample quality was checked by x-ray diffraction at room temperature. In the starting compounds $Y(Mn_{1-x}Al_x)_2$, the lattice constant slightly increases with the Al content x, as expected from the substitution of Mn by a bigger ion (Fig. 1). All the hydrides have a much higher lattice constant than the starting compounds, as expected from the insertion of hydrogen in all possible interstitial sites. Since the affinity of Al for hydrogen is low, in the

0163-1829/2000/62(14)/9493(5)/$15.00

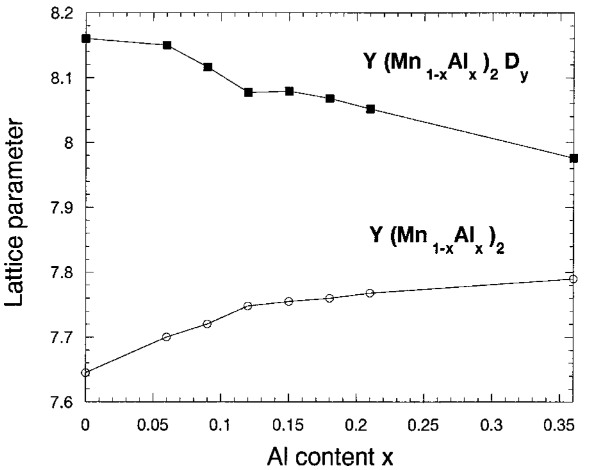

FIG. 1. Lattice parameter versus Al concentration x in $Y(Mn_{1-x}Al_x)_2$ and $Y(Mn_{1-x}Al_x)_2D_y$.

studied hydrides the maximal D content decreases with x (Table I), and consequently the lattice constant also decreases. We have limited our neutron study to Al substitutions with $x \leq 0.21$, which correspond to H contents in the range $y = 4 \pm 0.3$. In this range, the antiferromagnetic phase of the YMn_2H_y hydrides is stable.[13] The alloy with the lowest Al content ($x = 0.05$) showed an inhomogeneous mixture of two crystal phases at low temperature, so it was not considered in the analysis.

The Al content and the random distribution of Al on the Mn sites were checked by neutron diffraction. The large contrast between Al and Mn scattering lengths of similar amplitudes and opposite signs was a useful tool. We found that the Al concentration was the expected one, and that Al distribution was random.

III. NEUTRON POWDER DIFFRACTION

Neutron experiments were carried out *versus* temperature on the G61 powder diffractometer of the LLB using a large incident wavelength of 4.734 Å. The high luminosity of the spectrometer in the scattered q range ($0 < q \leq 2.5$ Å^{-1}) is especially suitable to an accurate determination of the magnetic order. Additional measurements with a shorter wavelength (1.593 Å) were also performed at some selected temperatures above and below the magnetic transition on the high-resolution diffractometer D2B of ILL. This allowed a full determination of the crystal structure. All spectra were refined using the FULLPROF program.[19]

TABLE I. Magnetic moment M_{Mn} measured at 10 K, Néel temperature T_N, and correlation length L_c for the $Y(Mn_{1-x}Al_x)_2D_y$ compounds. Error bars are mentioned in units of the last digit.

x	y	M_{Mn} (μB/Mn atom)	T_N (K)	L_c Å
0	4.3	3.2 (1)	340 (5)	>500
0.09	4.42	2.5 (1)	200 (5)	18.4
0.12	4.13	2.3 (1)	175 (5)	18.2
0.15	3.89	1.9 (1)	150 (7)	18.0
0.21	3.72	1.7 (1)	125 (10)	17.2

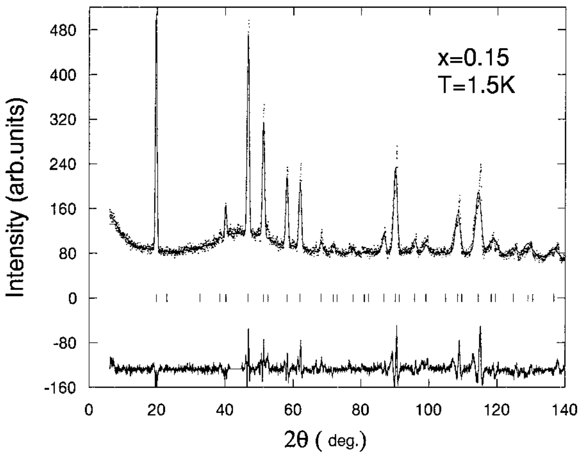

FIG. 2. Neutron-diffraction spectrum in the compound $Y(Mn_{1-x}Al_x)_2D_y$ ($x = 0.15, y = 3.89$), measured on the D2B diffractometer ($\lambda = 1.593$ Å) at 2 K. Bragg lines come from the structural order only. The diffuse peak around 46° is associated with short-range correlations between D atoms. The magnetic scattering is not visible on this scale and is included as a background in the structural refinement. Experiment (●), calculated spectrum (full line) and difference spectrum (full line in bottom). The tick marks show the positions of the structural peaks.

A. Crystal structure and hydrogen order

For all the studied Al contents, the diffraction spectra are indexed in a cubic symmetry down to the lowest measured temperature. The persistence of the cubic symmetry whatever the temperature contrasts with the case of the undoped hydride $YMn_2D_{4.3}$, where the cubic structure is observed in the disordered phase only, and a rhombohedral distortion occurs at the ordering transition. A typical spectrum is shown in Fig. 2. The Bragg peaks of the crystal structure have the same linewidth as in the intermetallic compounds, suggesting a homogeneous deuterium distribution. Below the Bragg peak of the crystal structure, a very broad and strong diffuse peak is observed around $2\theta = 46°$. This peak is attributed to short-range correlations between hydrogen atoms in the interstitial sites, which appear because the repulsive H-H interactions impose a minimum distance ($d = 2$ Å) between hydrogen neighbors.[15] These correlations are temperature independent.

The above features suggest that in the Al-substituted samples, hydrogen remains disordered in average at all temperatures. Therefore, we refined the chemical structure assuming a random hydrogen distribution on the A2B2 interstitial sites, and obtained good fits (Fig. 2), with reliability factors R_B around 6%.

B. Magnetic order

In all samples, the long-range magnetic order is broken by Al substitution, since no magnetic Bragg lines appear down to the lowest temperature. A diffuse peak is observed at the position of the 1/2 1/2 1/2 peak (Fig. 3). Its intensity strongly decreases with increasing temperature and disappears at the Néel transition, whereas its width remains temperature inde-

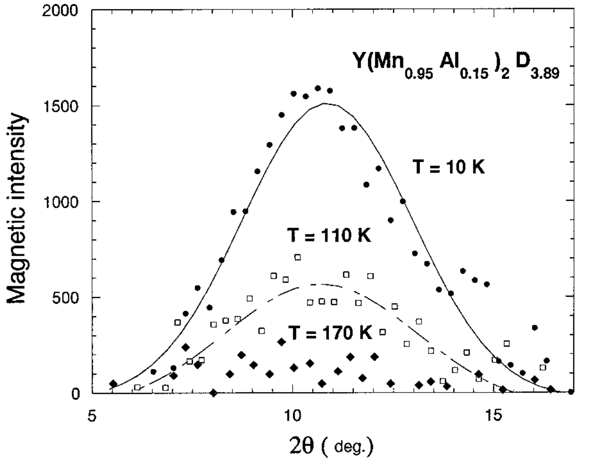

FIG. 3. Magnetic diffuse scattering of the compound $Y(Mn_{1-x}Al_x)_2D_y$ $(x=0.15, y=4\pm0.3)$, measured on the G61 diffractometer $(\lambda=4.734$ Å) for several temperatures. The sample background of a spectrum measured just above the Néel temperature was subtracted.

pendent within the precision of measurements. The magnetic transition is not associated with any structural change, nor with any anomaly of the lattice constant. To analyze the magnetic order, we have refined the spectra measured on G61 by assuming the same type of magnetic order as in the long-range-ordered structure of $YMn_2D_{4.3}$, corresponding to a $++--$ piling of ferromagnetic Mn planes along the 111 axis. The propagation vector was refined but remained always very close to the vector $\mathbf{k}=1/2\,1/2\,1/2$ of the long-range ordered structure. The Mn moments were constrained in the (111) plane (along the 2-1-1 direction), as for $YMn_2D_{4.3}$. The calibration of the integrated magnetic intensity with respect to that of the Bragg peaks of the crystal structure allows to determine an average value for the short-range ordered Mn moment.

The Mn moments are ordered over a length scale whose value is directly related to the inverse width of the magnetic peak, the influence of the instrumental resolution being negligible in this case. An accurate determination of the correlation length requires us to assume some model for the correlation function and therefore for the peak shape. We have tried two usual types of functions to model the peak shape, Gaussian and Lorentzian, respectively. The Gaussian shape gave the best adjustment (Rm = 6% compared to 9% in the Lorentzian case). The peak width was adjusted at low temperature where the magnetic intensity is maximum, then its value was kept constant to refine the spectra at higher temperatures. Under the very crude assumption of small ordered magnetic domains similar to chemical clusters, the domain size L_c is connected to the width H of the Gaussian magnetic peak [full width at half maximum (FWHM) expressed in radians] by the relation $L_c=\lambda/(\mathrm{H}\cos\theta)$ where 2θ is the scattering angle at the peak position.[20] The correlation length deduced from this relation (Table I) is around 18 Å which corresponds to a correlation of about 8 Mn planes along the 111 axis. In the Lorentzian model, which could be more realistic since it assumes an exponential decay of the correlation function, the correlation length has a little smaller value of 16 Å. It decreases only slightly with increasing Al content.

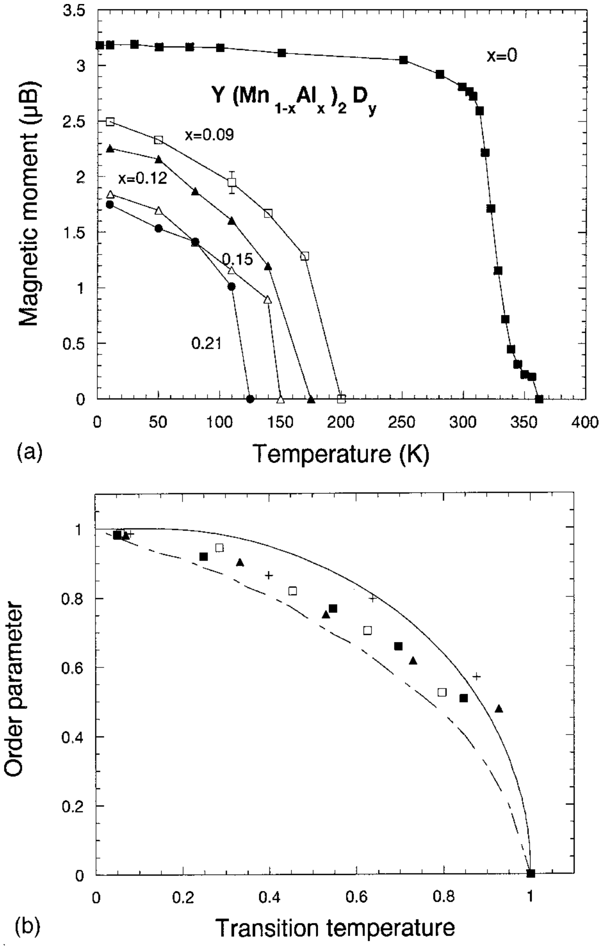

FIG. 4. (a) Temperature dependence of the Mn moments. (b) Magnetic moment M/M_0 versus temperature T/T_0 in reduced units in $Y(Mn_{1-x}Al_x)_2D_y$. M_0 and T_0 are the magnetic moment at low temperature and the transition temperature, respectively. (■) $x=0.09$, (□) $x=0.12$, (▲) $x=0.15$, (+) $x=0.21$. The lines are mean-field calculations of the order parameter. The solid line indicates ferromagnetic order parameter with the spin value for the Mn^{3+} ion, deduced from the Brillouin function with $J=2$. The dashed line indicates the spin-glass order parameter $q^{1/2}(T)$, where q is the Edwards–Anderson parameter, as calculated in Ref. 21.

The temperature dependence of the Mn moments are reported in Fig. 4(a). Even for the lowest Al context $x=0.09$, we observe important differences with the behavior in $YMn_2D_{4.3}$. The Néel temperature is strongly reduced, together with the moment value at low temperature. Moreover the curve shape is also modified. In $YMn_2D_{4.3}$, the Mn moment shows a steplike decrease in the vicinity of T_N, then it remains almost constant down to the lowest temperature. This is the signature of a first-order transition, which coincides with the order-disorder transition of hydrogen in the interstitial sites. In contrast, in the Al-doped samples where hydrogen remains disordered at all temperatures, the Mn moments increase smoothly with decreasing temperature, as for a second-order transition. When they are plotted in reduced units, the thermal variations of the moments measured for all Al contents collapse on a single curve [Fig. 4(b)]. In comparison, we have plotted the order parameters calculated by mean-field models for a nonfrustrated ferromagnetic order

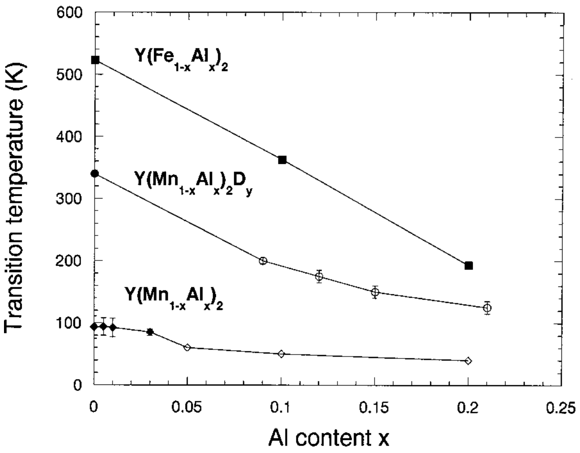

FIG. 5. Transition temperatures versus Al content in $Y(Mn_{1-x}Al_x)_2D_y$ (○) this work, (●) from Ref. 15, $Y(Mn_{1-x}Al_x)_2$ (◆) from Ref. 8; (◇) from Ref. 7, and $Y(Fe_{1-x}Al_x)_2$ (■) from Ref. 23. Full symbols correspond to a long-range ordered phase (correlation length L_c greater than several hundreds of Å), and open symbols to a short-range ordered spin-glass-like one (correlation length L_c of about 20 Å).

and for a fully frustrated spin glass order, in the infinite range Ising model.[21] The experimental curve lies in between these two extreme cases.

IV. DISCUSSION

A. Al substitution and H disorder

Even a very small Al content induces hydrogen disorder. This effect is related to the low affinity of Al for hydrogen, and to the fact that Al and H modify the electronic structure in the same way by creating low-energy states. As mentioned above for $YMnD_{4.3}$, hydrogen ordering controls the magnetic ordering, because it releases the topological frustration by modifying some specific Mn-Mn interactions. Therefore, the onset of hydrogen disorder induced by Al is the primary effect which modifies Mn magnetism.

B. Al defects in a frustrated lattice: comparison between $Y(Mn_{1-x}Al_x)_2D_y$, $Y(Mn_{1-x}Al_x)_2$ and $Y(Fe_{1-x}Al_x)_2$

We first compare the Al doping in $Y(Mn_{1-x}Al_x)_2$ and in the studied hydrides. The undoped compounds YMn_2 and $YMn_2D_{4.3}$ both show a long-range magnetic order. In YMn_2 this magnetic order is incommensurate and stabilized by lattice distortions, whereas in $YMn_2D_{4.3}$, it is commensurate and induced by hydrogen order. In both compounds, a small amount of Al (about 5%) substituted in the Mn sublattice strongly decreases the ordering temperature, and induces a short-range ordered state similar to a spin glass, with a correlation length of about 20 Å in both cases. A further increase of Al concentration no longer changes the qualitative behavior. This is shown in Fig. 5, where the transition temperatures are plotted versus Al content in the two systems. In $Y(Mn_{1-x}Al_x)_2$ the effect of Al substitution[5–7] was explained using the model of Villain[11] for topologically frustrated systems. Namely, a few defects randomly distributed in the frustrated pyrochlore lattice couple all spins and induce a spin-glass order. In the hydrides studied here, Al defects mostly act by inducing hydrogen disorder. From the results of Ref. 15, we expect that H doping strongly modifies Mn-Mn interactions. Therefore, the effective concentration of defects induced by Al disorder should be much higher than the nominal Al content. This explains the rapid breakdown of the long-range order observed in the hydrides with increasing Al content. The transition temperatures towards the disordered phase remain much higher than for the intermetallic compounds. These hydrides are among the most concentrated ‘‘spin glasses’’ ever observed, with a magnetic ordering temperatures as high as 200 K for $x=0.9$.

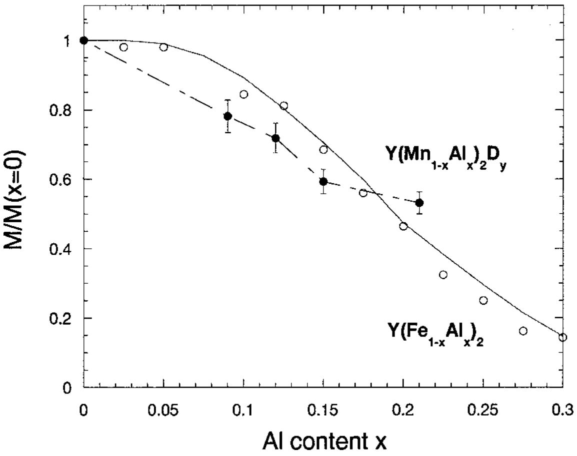

FIG. 6. Magnetic moment measured at 10 K versus Al content in $Y(Mn_{1-x}Al_x)_2D_y$ (●) this work and in $Y(Fe_{1-x}Al_x)_2$ (○) from Ref. 25. The solid line is the calculation given by the local environmental model of Ref. 25.

It is interesting to compare the effect of dilution in a frustrated lattice with that in a nonfrustrated one. The $Y(Fe_{1-x}Al_x)_2$ compounds[22–24] have the same Laves structure but the first-neighbor interactions are ferromagnetic. So, there is no topological frustration. A competing interaction could only come from farther neighbor magnetic pairs. Here, the long-range ordered phase and the spontaneous magnetization are preserved up to a much higher Al content (about 30% Al), with the transition temperature decreasing linearly with Al doping (Fig. 5). The magnetic phase diagram[24] is similar to that observed in many reentrant spin glasses, independently of the crystal structure.

C. Localized and itinerant magnetism: Mn moments in $Y(Mn_{1-x}Al_x)_2D_y$ and $Y(Fe_{1-x}Al_x)_2$

In both systems the Mn moment at low temperature strongly decreases with Al content (Fig. 6). Such a decrease could have two possible origins; (i) a reduction of the ordered moment with respect to the local one due to magnetic disorder; (ii) an intrinsic decrease of the local moment. The first effect is likely preponderant in the hydrides which are strongly disordered, but with a Mn-Mn distance (2.9 Å) well above the critical one (2.7 Å), so that the moments should be localized. The second effect dominates in $Y(Fe_{1-x}Al_x)_2$ where there is no topological frustration, but the moments are close to the instability limit. In this system, the decrease of average Fe moment with Al content was explained assuming a collinear order, the length of a given Fe moment depending on the number of its Al close neighbors.[25] The change of the local density of state associated with this effect comes from the hybridization of the *d* Fe orbitals with the *p* Al orbitals.[26] In contrast, in the present hydrides the length of the local Mn moment should not depend much on the local environment, but its orientation locally varies due to the hydrogen disorder. Neutrons only probe the correlated spins. Randomly disordered spins or spin components contribute only as a background in the diffraction spectra, so that the ordered moment is reduced with respect to the local one.

V. CONCLUSION

Al dilution strongly affects the magnetic properties of the Laves hydrides YMn_2D_4. The transition temperature strongly decreases and the long-range magnetic order is broken even for very low Al content. This effect may be associated to the onset of H disorder. In contrast with YMn_2, $Y(Mn_{1-x}Al_x)_2$, and $Y(Fe_{1-x}Al_x)_2$, the $3d$ moments remain fully localized, due to the large lattice expansion induced by both H and Al atoms.

---

[1] R. Ballou, J. Deportes, R. Lemaire, Y. Nakamura, and B. Ouladiaf, J. Magn. Magn. Mater. **70**, 129 (1987).

[2] R. Cywinski, S. H. Kilkoyne, and C. A. Scott, J. Phys.: Condens. Matter **3**, 6473 (1991).

[3] T. Freltoft, P. Bni, G. Shirane, and K. Motoya, Phys. Rev. B **37**, 3454 (1991).

[4] J. Deportes, B. Ouladiaff, and R. A. Ziebeck, J. Magn. Magn. Mater. **70**, 14 (1987).

[5] M. Shiga, Physica B **149**, 298 (1988).

[6] M. Shiga, H. Wada, K. Yoshimura, and Y. Nakamura, J. Magn. Magn. Mater. **54-57**, 1073 (1986).

[7] K. Motoya, J. Phys. Soc. Jpn. **55**, 3733 (1986).

[8] I. S. Dubenko, I. Yu. Gaidukova, Y. Hosokoshi, K. Inoue, and A. S. Markosyan, J. Magn. Magn. Mater. **195**, 687 (1999).

[9] K. Motoya, T. Freltoft, P. Böni, and G. Shirane, Phys. Rev. B **38**, 4796 (1988).

[10] K. Motoya, S. M. Shapiro, L. Rebelsky, and M. S. Torikachvili, Phys. Rev. B **44**, 183 (1991).

[11] J. Villain, Z. Phys. B **33**, 31 (1978).

[12] M. Pajda, R. Aruja, B. Johansson, J. M. Wills, H. Figiel, A. Paja, and O. Eriksson, J. Phys.: Condens. Matter **8**, 3373 (1996).

[13] J. Przewoznik, J. Zukrowski, and K. Krop, J. Magn. Magn. Mater. **140-144**, 807 (1995).

[14] H. Figiel, J. Przewoznik, V. Paul-Boncour, A. Lindbaum, E. Gratz, M. Latroche, M. Escone, A. Percheron-Guegan, and P. Mietniowski, J. Alloys Compd. **274**, 29 (1998).

[15] I. N. Goncharenko, I. Mirebeau, A. V. Irodova, and E. Suard, Phys. Rev. B **56**, 2580 (1997).

[16] I. Mirebeau, I. N. Goncharenko, A. V. Irodova, and E. Suard, Physica B **241-243**, 672 (1998).

[17] I. N. Goncharenko, I. Mirebeau, A. V. Irodova, and E. Suard, Phys. Rev. B **59**, 9324 (1999).

[18] K. Fujiwara, J. Phys. Soc. Jpn. **57**, 2133 (1988).

[19] J. Rodriguez-Carvajal, Physica B **192**, 55 (1993).

[20] A. Guinier, *Théorie et Technique de la Radiocristallographie*, 2nd ed. (Dunod, Paris, 1956).

[21] S. Kirkpatrick and D. Sherrington, Phys. Rev. B **17**, 4384 (1978).

[22] K. H. J. Buschow, J. Less-Common Met. **40**, 361 (1975).

[23] R. Grossinger, W. Steiner, and K. Krec, J. Magn. Magn. Mater. **2**, 196 (1976).

[24] G. Hilsher, J. Magn. Magn. Mater. **27**, 1 (1982).

[25] M. J. Besnus, J. M. Bouton, R. Clad, and A. Herr, Physica B **86-88**, 85 (1977).

[26] H. Yamada and M. Aoki, J. Magn. Magn. Mater. **104-107**, 1967 (1992).